University of Massachusetts Amherst

ScholarWorks@UMass Amherst

Masters Theses   Dissertations and Theses

November 2016

Characterizing the Inhibition of Katanin Using Tubulin Carboxy-Terminal Tail Constructs

Corey E. Reed
University of Massachusetts Amherst

Follow this and additional works at: https://scholarworks.umass.edu/masters_theses_2

Part of the Biochemistry Commons, Biophysics Commons, and the Molecular Biology Commons

Recommended Citation

Reed, Corey E., "Characterizing the Inhibition of Katanin Using Tubulin Carboxy-Terminal Tail Constructs" (2016). *Masters Theses*. 441.
https://scholarworks.umass.edu/masters_theses_2/441

CHARACTERIZING THE INHIBITION OF KATANIN USING TUBULIN CARBOXY-TERMINAL TAIL

CONSTRUCTS

A Thesis Presented

by

COREY E. REED

Submitted to the Graduate School of the

University of Massachusetts Amherst in partial fulfillment

of the requirements for the degree of

MASTER OF SCIENCE

SEPTEMBER 2016

Molecular and Cellular Biology

CHARACTERIZING THE INHIBITION OF KATANIN USING TUBULIN CARBOXY-TERMINAL TAIL

CONSTRUCTS

A Thesis presented

by

COREY E. REED

Approved as to style and content by:

_____

Jennifer Ross, Chair

_____

Thomas Maresca, Member

_____

Peter Chien, Member

_____

Elizabeth R. Dumont, Director

Interdepartmental Graduate Programs, CNS

ABSTRACT

CHARACTERIZING THE INHIBITION OF KATANIN USING TUBULIN CARBOXY-TERMINAL TAIL

CONSTRUCTS

SEPTEMBER 2016

COREY E. REED

B.S., UNIVERSITY OF MASSACHUSETTS AMHERST

M.S., UNIVERSITY OF MASSACHUSETTS AMHERST

Directed by: Dr. Jennifer L. Ross

Understanding how the cellular cytoskeleton is maintained and regulated is important

to elucidate the functions of many structures such as the mitotic spindle, cilia and flagella.

Katanin p60, microtubule-severing enzymes from the ATPase associated with cellular activities

(AAA+) family, has previously been shown in our lab to be inhibited by free tubulin as well as α-

and β-tubulin carboxy-terminal tail (CTT) constructs. Here we investigate the inhibition ability of

several different tubulin CTT sequences. We quantify the effect of the addition of these

constructs on the severing and binding activity of katanin. We find that some constructs inhibit

katanin better than others and two constructs that appear to enhance katanin activity. Our

findings add nuance to our previous findings that consensus α-tubulin tails are less inhibitory of

katanin than consensus β-tubulin [3]. Surprisingly, we find that a polyglutamate sequence

activates katanin while it has previously been shown to inhibit spastin, a different microtubule-

severing enzyme associated with the neuromuscular disease Hereditary Spastic Paraplegia [23].

These results highlight that different CTT sequences can control the activity of severing

enzymes and ultimately affect the cytoskeletal network organization in a cell type and location-

dependent manner.

TABLE OF CONTENTS

LIST OF FIGURES

CHAPTER 1

INTRODUCTION

One of the most important cellular systems in biology is the cytoskeleton. This system provides the cell with structure, acts as a pathway for protein transport within the cell and is responsible for key processes such as cell division. A major component of the cellular cytoskeleton is the tube-like assembly of proteins called the microtubule. Microtubules are
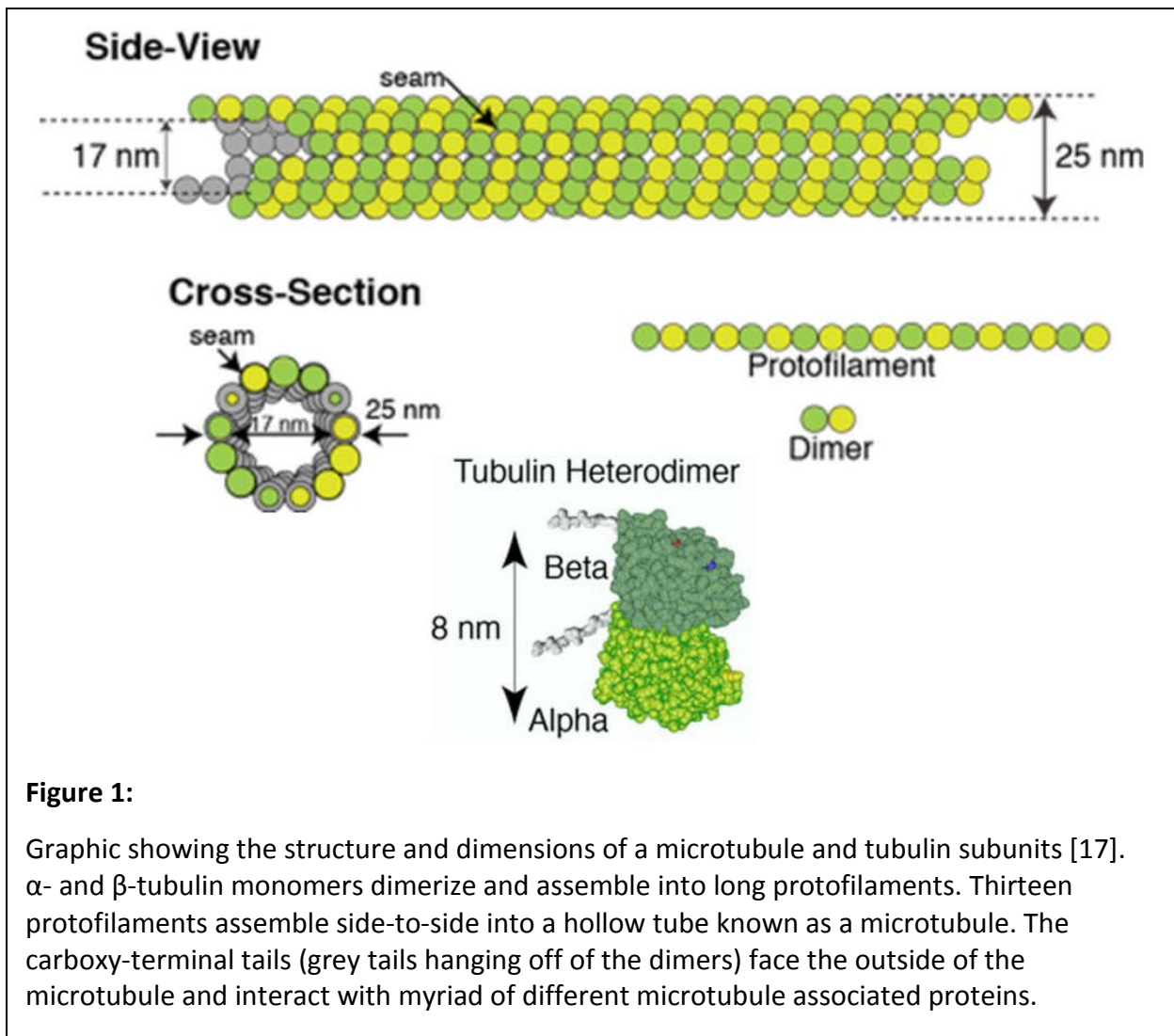
Figure 1:

Graphic showing the structure and dimensions of a microtubule and tubulin subunits [17]. α- and β-tubulin monomers dimerize and assemble into long protofilaments. Thirteen protofilaments assemble side-to-side into a hollow tube known as a microtubule. The carboxy-terminal tails (grey tails hanging off of the dimers) face the outside of the microtubule and interact with myriad of different microtubule associated proteins.

formed from 55kD α- and β-tubulin monomers which dimerize and are highly conserved

throughout eukaryotes [1]. Dimers assemble end-to-end into protofilaments, which nucleate a canonical 13 protofilament structure assembled into a hollow tube, which is a microtubule (Figure 1).

When a microtubule is formed, the carboxy-terminal tail (CTT) of each tubulin monomer is facing out, allowing for microtubule-associated proteins (MAPs) to interact with the CTT. The carboxy-terminal tail of tubulin cannot be visualized through crystallographic methods because it is an intrinsically disordered region which is highly negatively charged. The sequence of α- and β-tubulin tails is highly variable and important for determining the role of the microtubule as a whole. The possibilities of "messages" to be created through this "microtubule code" of carboxy-terminal tails can be altered and amplified through post-translational modifications such as polyglutamylation and detyrosination, to name a few.

Microtubules are a part of the cellular cytoskeleton that give structure to the cell and form structures such as flagella and cilia. During cell division microtubules assemble into the mitotic spindle and, with the help of various microtubule associated proteins, work to separate the chromosomes [6, 11, 19]. Microtubules are dynamic building blocks that are constantly undergoing rounds of depolymerization (catastrophe) and subsequent polymerization (rescue) [3]. Small molecule drugs, such as paclitaxel (Taxol), stabilize microtubules reducing the frequency of catastrophes resulting in a static structure.

Microtubule dynamics are naturally tuned through microtubule-associated proteins and enzymes. Many MAPs stabilize microtubules, such as the tau protein found in the axons of nerve cells. Enzymes are needed to destroy the microtubule. One family of microtubule-

destroying enzymes are the microtubule-severing enzymes. Microtubule-severing enzymes consist of an enzymatic domain from the ATPases associated with various cellular activities (AAA+) family. There are three known types of microtubule-severing enzymes: fidgetin, spastin and katanin. These severing enzymes play a key role in maintaining complex microtubule arrays such as those found in the neurons, cilia and spindles of dividing cells [19]. Severing enzymes function by disrupting the noncovalent bonds between tubulin dimers using ATP hydrolysis [6]. Loss of function of any one of these enzymes leads to microtubule disarray in these important cellular structures and can lead to diseases such as hereditary spastic paraplegia [19, 23].

Katanin was the first discovered in Xenopus mitotic egg extract and was determined during this same study to be regulated along with the start of cell division through introduction of cyclin [22]. Surprisingly, katanin has not been well studied due to the difficulties in purifying and working with this protein. It is important that a clearer understanding of how katanin is regulated be achieved as it has many important roles including releasing microtubules from centrosomes, powering poleward flux at the mitotic spindle and accelerating the microtubule turnover rate [3, 10, 11, 19].

Katanin is actually made of two distinct subunits: p60 and p80, which are 60 and 80kD in size, respectively. Katanin p60 is the enzymatic region responsible for severing. Katanin p80 has WD propeller repeats that help to target and localize katanin p60 in the cell. In this thesis, we will only use p60 and refer to it simply as katanin.

Based on prior studies with spastin, we assume that the katanin p60 subunit

oligomerizes around the C-terminal tail of a tubulin monomer, threading it through the

hexameric ring where the ATPase may act [15] (Figure 2). Previous work with spastin has shown

that two loops located within the active pore of many AAA enzymes are essential for

interaction with the substrate. It is known that the first poor loop engages the target protein

and translocates it into the pore while the second poor loop, when mutated, disrupts substrate

binding [24]. It has previously been shown in our lab that removing the CTT of tubulin through

treatment with subtilisin prevents severing of the microtubule [3].

Figure 2:

Left: Spastin structure as determined by crystallography and small angle x-ray scattering
(SAXS) [15]. There is a pore in the center through which tubulin's carboxy-terminal tail is
threaded. Right: A schematic of how katanin could interact with the surface of the
microtubule.
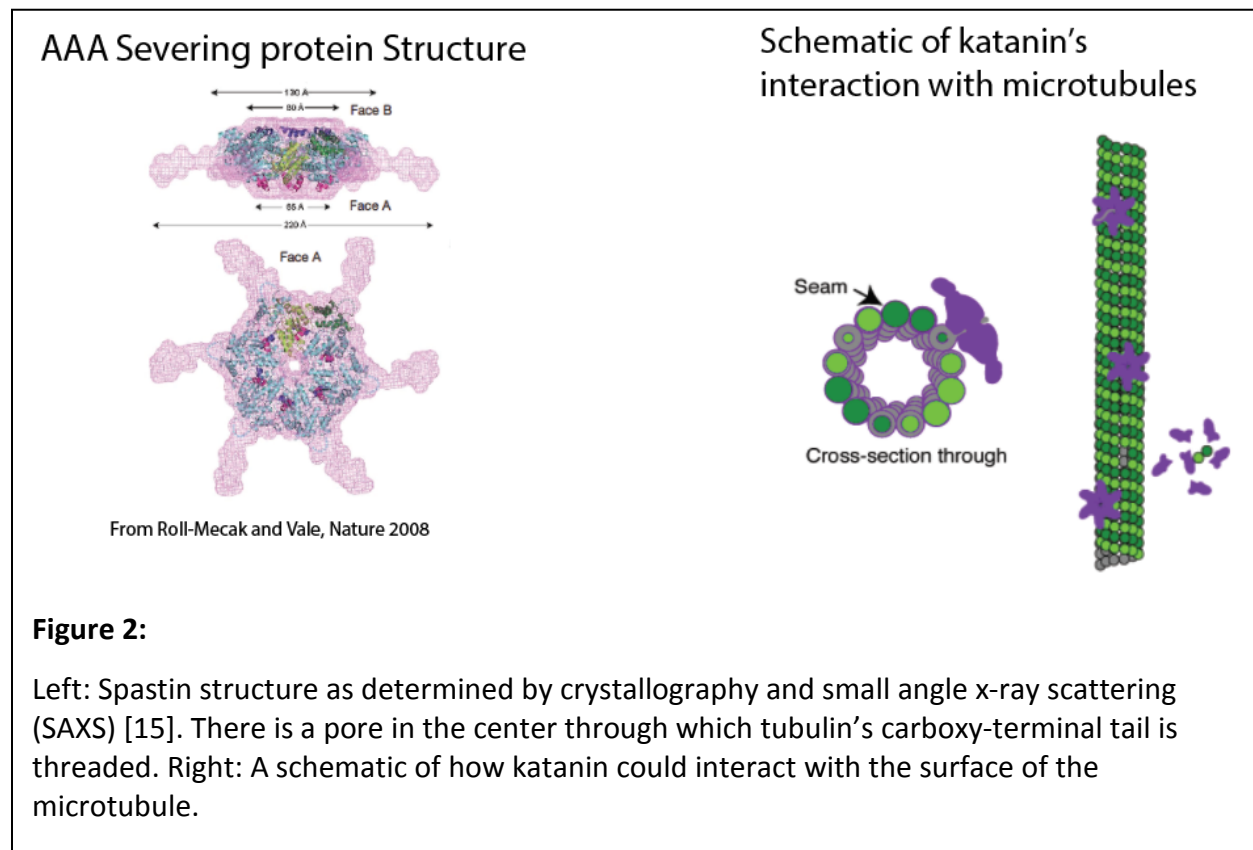
Katanin can destroy microtubules, yet we do not see whole-sale destruction in cells. It is implied that its activity must be regulated and shut down. We have shown previously that katanin severing and binding is inhibited in the presence of free tubulin. Further, we showed that the inhibition was controlled by only the CTT of tubulin. Using a novel CTT construct covalently bound to bovine serum albumin (BSA), we could test individual sequences for activity. We saw that the sequence of the CTT was able to regulate katanin activity [3] (Figure

Figure 3:

Microtubule severing by katanin is inhibited in the presence of free tubulin and BSA-tubulin C-terminal tail constructs [3]. Microtubules only are dark blue, microtubules with 50nM katanin are pink, microtubules with 50nM katanin and 50nM tubulin are light blue, microtubules with 50nM katanin and 50nM β-CTT are orange, microtubules with 50nM katanin and 50nM α-CTT are green and microtubules with 50nM katanin and 50nM detyrosinated α-CTT are purple. Colors in the left graph correspond to the tests described in the legend in the right graph. Notably, katanin alone severs much faster than in the presence of free tubulin or any of the CTT constructs tested.

3). This is important and interesting because it sets up a model of katanin regulation wherein there is a negative feedback loop to shut down severing after enough dimers have been released.

In this thesis, I have sought to better understand how the amino acid sequence of tubulin C-terminal tails, as well as the modifications added to them post translationally, affect katanin severing activity and binding rates. It has previously been shown that tubulin C-terminal tail modifications such as polyglutamylation can have a graded control on binding and severing activity of the severing enzyme spastin [23]. I expect that different modifications of the C-terminal tails of tubulin will result in differing rates of inhibition of katanin severing activity as well as changes in binding rate of katanin to the microtubule depending on the modification used.

Understanding how tubulin modifications affect binding and severing by katanin will allow for a more in depth look at how important structures within the cell are maintained and manipulated (e.g. the mitotic spindle and neuronal axons), as well as how inhibition is controlled within the cell. A clearer understanding of how this cellular mechanism is controlled will give us insight into how neurodegenerative diseases arise and potentially lead to new avenues for treatment.

CHAPTER 2

MATERIALS AND METHODS

2.1 Bacterial Katanin Purification

Optimized human p60 construct with a maltose binding protein and GFP (GeneWiz, Cambridge, MA) was transformed into BL21 competent *Escherichia coli* (New England BioLabs, Ipswich, MA). Colonies were allowed to grow and then added to 5mL of LB media with 1mM ampicillin as a starter culture the next day. Starter cultures were allowed to incubate at 37°C while shaking overnight. The following morning starter cultures were added to larger flasks of 400mL LB media containing 1mM ampicillin and allowed to shake in the 37°C incubator until an OD of 0.8 was reached. They were then induced with 1mM isopropyl β-D-1 thiogalactopyranoside and allowed to grow at 16°C while shaking for 14-16 hours. Following induction cells were pelleted and lysed in resuspension buffer (20mM HEPES-HCl, pH 7.7, 250mM NaCl, 0.5mM β-mercaptoethanol, 10% glycerol and 0.25mM ATP) using sonication. Lysate was incubated with amylose resin for 2 hours and the lysate-resin mixture was added to a column. Excess lysate was allowed to flow through the column completely and the lysate/resin bed was washed with 20mL resuspension buffer. Purified katanin was eluted from the column with 10mM maltose in resuspension buffer and the approximate concentration was determined using a Bradford assay.

2.2 Taxol-Stabilized Microtubule Polymerization

Taxol-stabilized microtubules were made by combining labeled HL 647 tubulin (Cytoskeleton, Denver, CO) or labeled rhodamine tubulin (Cytoskeleton, Denver, CO) with unlabeled tubulin purified from porcine brain in a 1:10 labeled/unlabeled ratio in PEM-100 (100mM K-PIPES, pH 6.8, 2mM $MgSO_4$ and 2mM EGTA) to a concentration of $5 \, mg/mL = 45 \, \mu M$. Tubulin was centrifuged at 360,000xg to remove aggregated tubulin. The supernatant with good tubulin was removed, GTP was added to 1mM, and placed at 37°C for 20 minutes to polymerize. Polymerized microtubules were stabilized with 50μM Taxol and incubated at 37°C for 20 minutes to equilibrate. The microtubule solution was then centrifuged at 14,000xg at 25°C and the pellet resuspended in PEM-100 with 50μM Taxol to clean up the microtubules.

2.3 Coverslip Silanization

Coverslip racks and glass containers were cleaned thoroughly before silanization. Coverslips were immersed in 100% acetone for 1 hour followed by an immersion in 100% ethanol for 10 minutes. Coverslips were then rinsed 3 times in ddH_2O for 5 minutes each time. Coverslips were then immersed in 0.1M KOH for 15 minutes which was prepared just before use. This was followed by another 3 washed in ddH_2O for 5 minutes. The coverslips were then allowed to air dry overnight while covered by tinfoil. The following day, once the coverslips were completely dry, they were immersed in 2% dimethyldichlorosilane for 5 minutes. This was followed by

immersion in 100% ethanol for 5 minutes 2 times. The coverslips were then rinsed 3 times in ddH_2O for 5 minutes each time and allowed to air dry while covered by tinfoil.

2.4 Severing Assay

A 10µL chamber was made using a silanized cover slip, a slide and double-sided tape such that buffers could be exchanged while imaging on the inverted chamber while on the microscope (Figure 4). First, 10µL of 2% rat α-tubulin antibody in PEM-100 was flowed into the chamber and incubated at room temperature for 5 minutes. Next, 10µL of 5% F-127 was flowed into the chamber and incubated at room temperature for 5 minutes. A 1:100 concentration of microtubules in PEM-100 with 50µM Taxol was prepared while waiting. Next, 10µL of the 1:100 microtubule mixture was added to the chamber and incubated at room temperature for 5
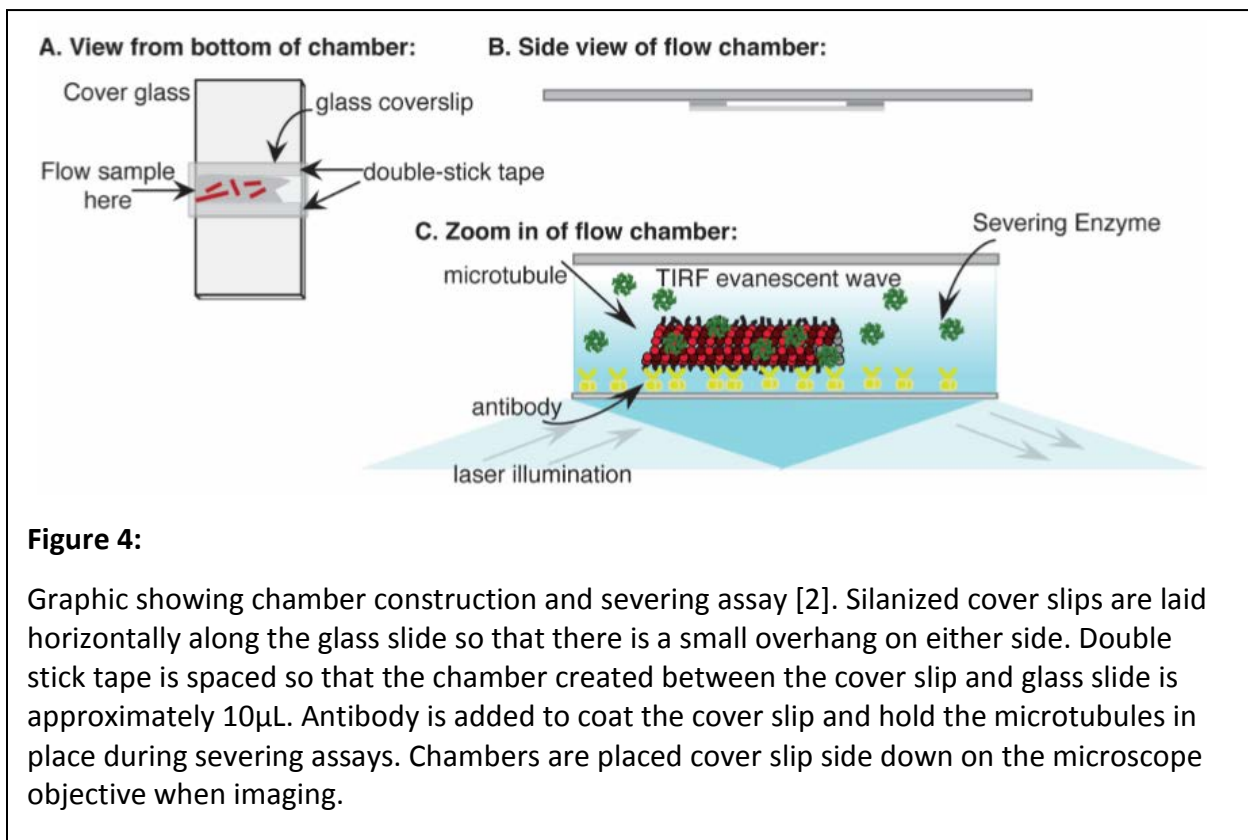
Figure 4:

Graphic showing chamber construction and severing assay [2]. Silanized cover slips are laid horizontally along the glass slide so that there is a small overhang on either side. Double stick tape is spaced so that the chamber created between the cover slip and glass slide is approximately 10µL. Antibody is added to coat the cover slip and hold the microtubules in place during severing assays. Chambers are placed cover slip side down on the microscope objective when imaging.

minutes. While waiting Katanin Activity Buffer (KAB) was prepared (20mM HEPES, 2mM $MgCl_2$, 10% Glycerol, 0.05% F-127, 50mM DTT, $5\,mg/mL$ BSA, 50μM Taxol, 2mM ATP, $15\,mg/mL$ glucose, $0.15\,mg/mL$ catalase, $0.05\,mg/mL$ glucose oxidase). 10μL of KAB was added to the chamber and immediately brought to image on the microscope. After imaging the microtubules in epi-fluorescence, GFP-katanin in KAB was added to the chamber with or without BSA-CTTs for testing and imaged using epi-fluorescence and total internal reflection fluorescence (TIRF) microscopy.

2.5 TIRF and Epi-Fluorescence Imaging

Videos were taken in two channels. Using a home-built total internal reflection fluorescence
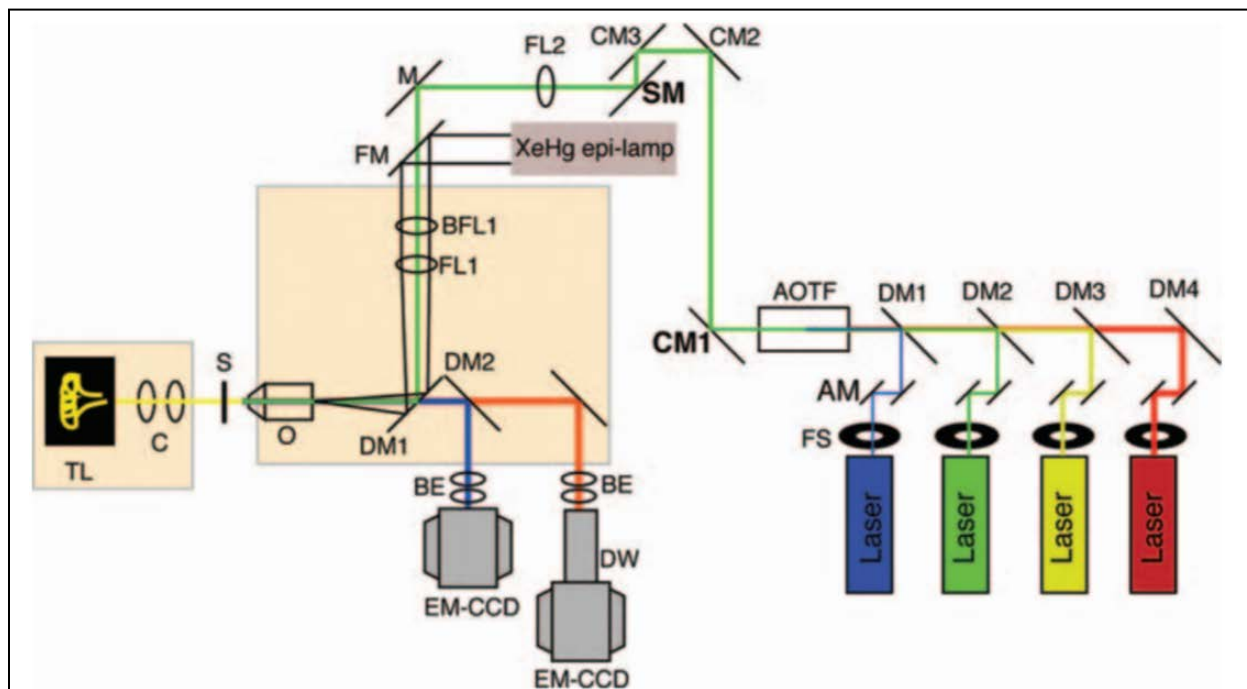
Figure 5:

Example of a multicolor TIRF setup [16]. M, mirror; CM, combination mirror; SM, steering mirror located at front focal plane conjugate; AM, aligning mirror; O, objective; S, sample; C, condenser; TL, transmitted light lamp; DM, dichroic mirror; FL, focus lens; BFL, back focus lens; FM, flip mirror; AOM, acousto-optical modulator; FS, fast shutter; BE, beam expander; DW, dual-wavelength splitting system; EM-CCD, electron multiplier CCD camera. Laser is aligned by passing transmitted light through the objective and out the laser port.

(TIRF) system (Figure 5) [16]. The microscope used was a Nikon Eclipse Ti running Nikon Elements with an Andor iXon3 camera. Microtubules were imaged using epi-fluorescence in either green or red illumination depending on if the microtubules were rhodamine or HL 647, respectively. Epi-fluorescence exposure time was 300ms and a time-lapse was recorded at 5 second intervals. Katanin was imaged in TIRF using a 488nm laser with 30ms exposure times and 5 second intervals. The video was allowed to run for approximately 30 seconds and the KAB containing reagents to be tested were flowed in and the video was allowed to run for the remainder of 10 minutes.

2.6 Video Analysis

Videos were analyzed using ImageJ. The two channels each video 9red epi-fluorescence and green TIRF) were split into different stacks. Each stack was run through a drift correction plugin (StackReg) to correct any drift throughout the video. A line was drawn through an individual microtubule and the average intensity over the entire length of the microtubule was measured through every frame in the stack using a plugin (MeasureStack). The line was then moved off of the microtubule to an area far enough away to measure the nearby background noise without overlapping any other microtubules. The data was exported as a text file to Microsoft Excel for analysis.

2.7 Spreadsheet Analysis

A new Microsoft Excel document was created for each video analyzed. In each document a separate sheet was created for each microtubule measured in that video. Each sheet contained both the epi-fluorescence and TIRF fluorescence intensity data for each microtubule. For epi-fluorescence (microtubule) data, signal was divided by background noise and subtracted by 1 to correct for background intensity. The background intensity was time dependent, so we made this correction for each time point for the measured average background intensity. The entirety of the data was normalized by averaging the points before introduction of reagents and dividing every data point throughout the video by this average. This made the initial intensity equal to 1 no matter if the microtubule was slightly brighter or dimmer initially. The microtubule intensity decay plot starts at 1 and decreases to zero if all polymer was lost. For TIRF (katanin) data, signal was divided by noise and 1 was subtracted, but the data was not normalized. This allowed us to observe the maximum level of katanin binding. Each microtubule measured was plotted in a decay graph to check for outliers. All data from the same conditions was averaged together in a separate document and a final decay graph of the overall trend was created.

2.8 Kaleidagraph Analysis

Kaleidagraph was used to fit decay data from Microsoft Excel to an exponential decay of the form:

$$I_{MT}(t) = I_{final} + I_0 * \exp(^{-t}/_{\tau}) \qquad \text{Eq. 1}$$

Where $I_{MT}(t)$ is the average intensity along the microtubule as a function of time, I_{final} is the

final intensity in the region of the microtubule, I_0 is the amplitude of the intensity decay and τ is

the characteristic decay time. Comparing the characteristic decay time (tau) for each test allows

us to compare activities from different experiments.

RESULTS AND DISCUSSION

3.1. Katanin Severing and Binding Activity Show Significant Prep-to-prep Variance

One of the more significant hurdles during testing of the different inhibitors was the

lifetime of katanin following purification. A day-long purification was performed immediately

followed by testing of katanin's severing under differing conditions. Due to variances in the

Figure 6:

Katanin severing activity and binding varies significantly between preps. Light blue corresponds to controls run on 10-1-2015, orange corresponds to controls run on 11-24-2015, grey corresponds to controls run on 12-17-2015, yellow corresponds to 100nM katanin controls run on 3-24-2016 and purple corresponds to 200nM katanin controls run on 3-24-2016. The left graph shows microtubule decay over time. The right graph shows maximum katanin binding over the entire microtubule over time. Both graphs were an average of all microtubules in all control videos during the date of experiment.

quality of the preparation and factors such as room temperature and the length of time the

purification process took, katanin would demonstrate different severing activities (Figure 6).

Both severing and binding data were measured using ImageJ to quantify the average

intensity over the entire microtubule through all frames of each video (please see Materials and

Methods). The intensity data on the microtubule (signal) was divided by the intensity of the

background near the microtubule (background) for each frame. The signal to noise ratio was

calculated and normalized for individual microtubules to account for location-specific intensity

changes within the chamber. The analysis is the same as previously published [3]. In addition to

quantifying the rate of severing, we also quantified the amount of GFP-katanin that bound to

the microtubule during severing, as previously done [3].

Due to the variability in activity, we performed the following tests each time. Before any

inhibition experiments were run control tests were performed to determine the appropriate

concentration of katanin to use for testing. The rate of katanin severing was best between 1 – 5

minutes to completely destroy all the filaments in the frame. After a good working

concentration was determined (typically 50 – 200nM, similar to previous preparations from

[3]), we would perform tests that could be compared to that day's control. We made sure to

test the control was still functioning at high activity throughout the day. We also altered the

order in which the tests were performed in order to stave off any ill effects due to loss of

activity over the course of the day. From the decay data we were able to determine which

constructs inhibited katanin the best.

3.2 The Carboxy-Terminal Tails of Tubulin are Highly Variable

We sought to test the effect of CTT sequence on the inhibition of katanin binding and severing. Although tubulin sequences are very similar between species [9], the CTT is a highly variable region. Further, the CTT is known to control the binding of microtubule-associated

Figure 7:

The construct maps for each BSA-tubulin CTT construct with color coded amino acids. Red letters indicate negatively charged amino acids. Green letters indicate polar amino acids. Blue letters indicate amino acids with aromatic rings. Purple letters indicate amino acids with a positive charge. Yellow letters indicate amino acids with a positively charged aromatic ring. β and α are consensus β- and α-tubulin CTT sequences. αΔY is a detyrosinated α-tubulin CTT. These three constructs were previously tested in our lab [3]. The remaining eight constructs were given to us by Dan Sackett for testing.

proteins and alter the activity of severing enzymes [3]. We have chosen to examine several

specific sequences of α- and β-CTTs that are found in specific cell types in the body. Tubulin

expressed from the gene TUBA1A (αδ2) are prominent in neurological cells along with those

expressed from TUBB2A (β2A) and TUBB3 (β3). Tubulin from the gene TUBB4B (β4B) are

expressed primarily in glandular cells. Tubulin from the gene TUBB1 (β1) are found in platelets

and megakaryocytes. Tubulin from the gene TUBB6 (β6) are found ubiquitously. To achieve a

better understanding of the differences between these tails, we took a closer look at the

chemical makeup of each construct (Figure 7).

Previous studies from our lab have shown that CTT constructs of β- and α-tubulin inhibit

katanin differently [3]. The consensus β-tubulin tail was the best inhibitor. This sequence

contains a bulky nonpolar aromatic group in the middle and a region of 5 negative charges in a

row. Comparing this to the consensus α-tubulin, the second best inhibitor of katanin, we see

that the α-tubulin has the bulky aromatic ring at the end of the CTT and no large region of

negative charge along its length. Lastly, the detyrosinated α-tubulin CTT was the worst inhibitor

of katanin in this study and had the bulky aromatic group removed from the end. Based off of

these results, we hypothesize that a lengthy region of negative charge as well as a bulky

aromatic group in the middle portion of the CTT could be important towards CTT binding to

katanin resulting in inhibition.

The new CTT constructs we are testing are similar in some ways to the consensus

tubulins and detyrosinated tubulin previously tested. Based on the new CTT sequences and our

model for what is good to inhibit katanin, we can make predictions based on the sequences we

are testing:

- The CTT αδ2 is similar to αΔY in length and contains no large negative region or aromatic rings. With this knowledge we predict αδ2 to be a poor inhibitor of katanin.

- The CTT β A+Y is large like the consensus β-tail previously tested and contains a large region of negative charge and 2 aromatic rings. The aromatic ring at the end of the CTT similar to the consensus α-tail previously tested leads us to predict that β A+Y should be a strong inhibitor of katanin.

- The CTT β2A has a large negative region with a bulky aromatic ring in the middle and as such we predict it will be a good inhibitor of katanin.

- The CTT β3 does have a large negative region and a bulky aromatic ring in the center, but it also has a positive charge and an aromatic ring at the end. Because of this aromatic ring at the end as well as the positive charge we predict that β3 will be a poor inhibitor of katanin.

- The CTT β4B has a few smaller regions of negative charge as well as an aromatic ring in the middle and we predict it will be a moderate inhibitor of katanin.

- The CTT β6 is similar to the consensus β tail previously tested with a large negative region and aromatic ring in the middle and should be a good inhibitor of katanin.

- The CTT β1 has a large negative region but has a positively charged aromatic ring at the end and as such should be a poor katanin inhibitor.

- We tested a polypeptide consisting of solely glutamates, E10, for katanin inhibition. Previous studies showing polyglutamylation inhibits spastin [19] leads us to predict that this tail should inhibit katanin. However, the construct does not have any resemblance

to an actual tubulin tail. This construct is effectively testing the inhibitory effects of a

polyglutamylated side chain hanging off of an actual tubulin CTT.

3.3 Sequences of the C-terminal Tail of Tubulin Affect Inhibition of Katanin Severing and

Figure 8:

Plots demonstrating one day of experiments testing four of the eight BSA-tubulin CTT constructs. The concentration of free tubulin and all BSA-tubulin CTT constructs is 50nM, the lowest concentration where severing inhibition by free tubulin was observed in previously published data [3]. Free tubulin can be treated as a control for inhibition levels. The left graph shows the differing rates of severing observed with 100nM of katanin in each test. From this we see a distinct profile for each inhibitor. It is interesting to note that β3 appears to not inhibit katanin at all while the other constructs inhibit on a comparable level to free tubulin. The right graph shows binding profiles of katanin under different severing conditions by plotting average katanin intensity bound along the microtubule as a function of time. Light blue corresponds to the control, orange corresponds to free tubulin tests, grey corresponds to β2A tests, yellow corresponds to αδ2 tests, and purple corresponds to β A+ Υ tests and green corresponds to β3 tests.

Binding

It was previously shown in our lab that free tubulin in solution with katanin inhibited
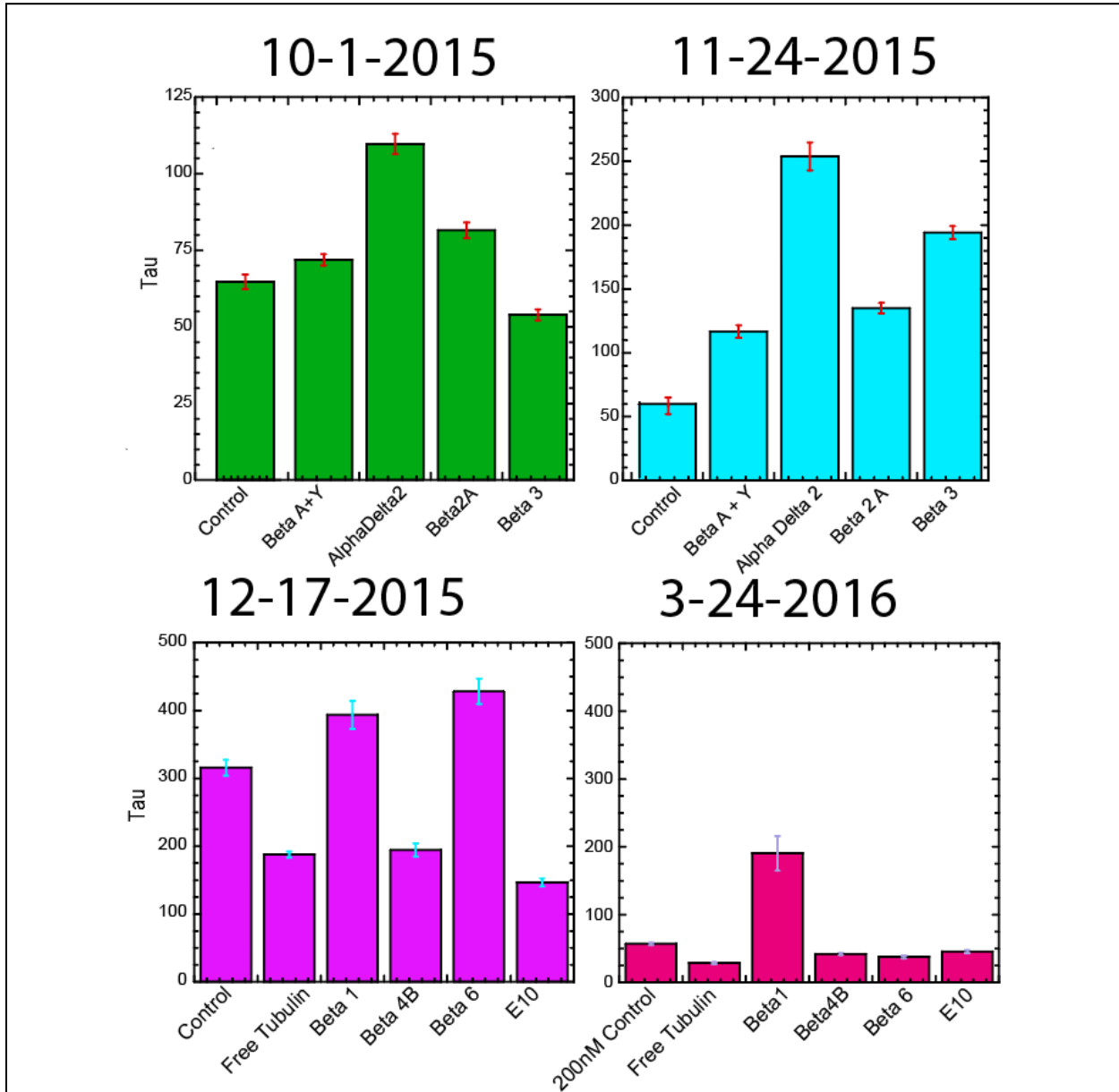
Figure 9:

Bar graphs of the average decay times (τ) for all BSA-tubulin CTT constructs as well as the control katanin concentration and free tubulin inhibition controls. All controls were run with 100nM of katanin unless otherwise indicated. All free tubulin and construct concentrations were 50nM. Preparation differences can be observed by comparing the control data between plots. We are interested in the trends due to the presence of BSA-CTT sequences.

severing at levels as low as 50nM [3]. This was demonstrated with both tubulin purified from porcine brain which consists of a mix of all CTT modifications and with CTT constructs connected to a BSA protein. From that study, it was clear that the CTT sequence affects the ability of katanin to bind and sever. We took a more in depth look at singular modifications of multiple beta- and one alpha-tubulin CTT in order to achieve a better understanding of how katanin activity is regulated (Figure 8).

Because of the variance in katanin activity, we analyzed the decay plots with a line of best fit given in equation 1 (Methods). Using the best-fit line, we can compare between preps for the same inhibitors (Figure 9).

For each preparation, we compare the decay times for each inhibitor to the same day control (Figure 8). We see that most of the inhibitor tests show the same trend in terms of decay time. αδ2, β A+Y, β2A, free tubulin, β1, β4B and E10 all show similar relations to the

Figure 10:

Bar-graphs showing the maximum level of katanin binding for each inhibitor on each day tested. Binding was measured by using the signal along the microtubule over the noise background noise near the microtubule (see materials and methods).
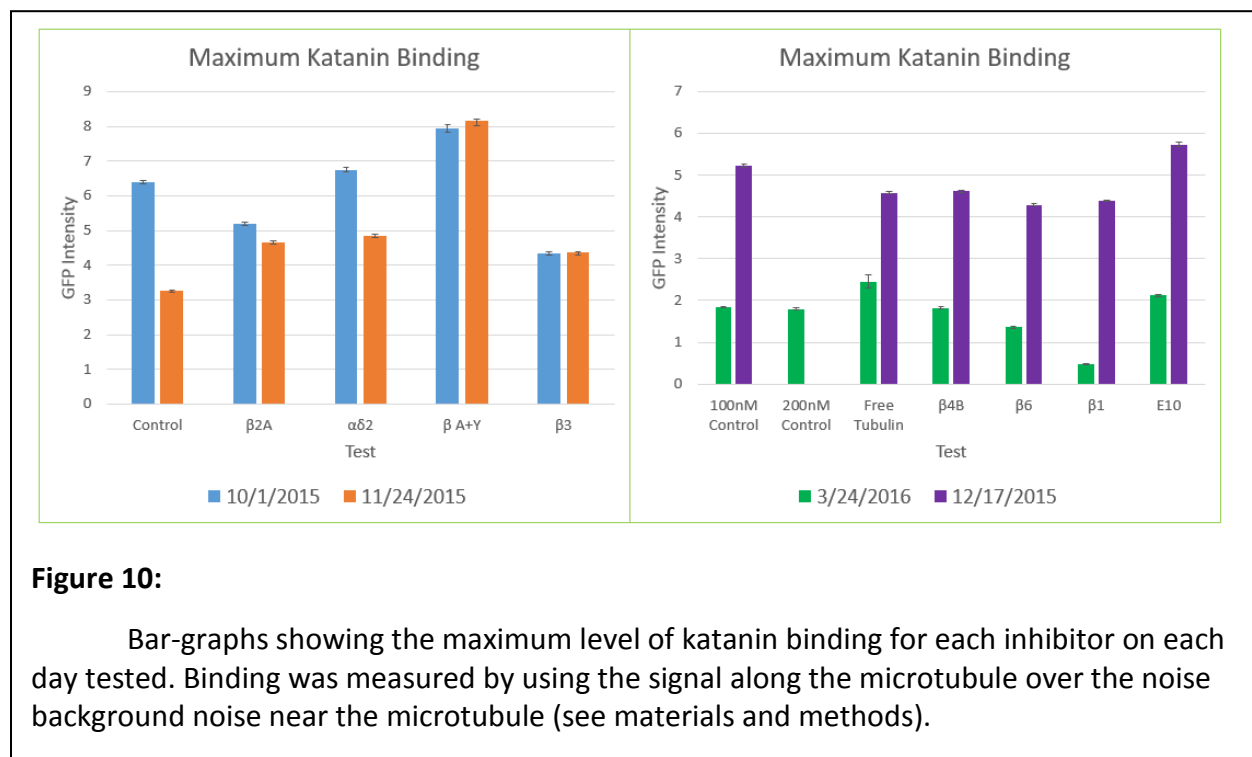
control decay time. Interestingly β6 and β3 show significantly different decay times between the two preparations. These inhibitors warrant further testing in the future to determine if these results were an artifact of human error.

The characteristic decay times inform on the severing rate, but we have a second measurement of katanin activity we quantify, the GFP katanin binding. Using TIRF microscopy to image in the green channel, we can visualize and quantify the binding of GFP-katanin to microtubules during the severing process. As previously shown, the GFP-katanin binding is proportional to severing activity [3]. We measured the GFP katanin maximal binding using ImageJ (Figure 10).

Figure 10 shows that each inhibitor tested affected binding in some way, but differently for different preparations. For example, β2A increased binding of katanin to the microtubule on 11/24/2015 but inhibited binding on 10/1/2015.

3.4 Carboxy-Terminal Tail Sequence Alters Katanin Severing Ability

Combining the construct maps in Figure 7 with the decay data from Figure 9, we can analyze what sequence features make a good inhibitor or causes activation and test our hypothesized results:

- The CTT αδ2 is intriguing as α-tubulin tails are reported to be less inhibitory towards katanin than β-tubulin tails [3]. However, we found that αδ2, the only α-tubulin tail tested, inhibited katanin more than any other. One possibility is that the CTT of the α-

tubulin is not what prevents katanin inhibition. Therefore, removing the bulk of the protein allowed the tail to interact with katanin in a way that it normally cannot, causing severe inhibition.

- The CTT β A+Y was previously predicted to be a good inhibitor of katanin because it contains a large region of negative charge and has an aromatic ring near the end of the CTT. This ended up being the case as it increased characteristic decay time of severing.

- The CTT β2A was predicted to be a good inhibitor of katanin because of the large negative region and aromatic ring in the middle of the CTT. This prediction is correct as β2A demonstrated good katanin severing inhibition ability.

- The CTT β3 presents an interesting case as it does contain a large negative region in the middle of the CTT but also has a large aromatic ring at the end as well as a positively charged amino acid. Results were mixed with this tail as it seemed to promote katanin severing on 10-1-2015 but severely inhibited katanin severing on 11-24-2015. This tail needs to be retested.

- The CTT β4B has several smaller regions of negative charge and a bulky aromatic ring in the center of the CTT. Our prediction that β4B would be a moderate inhibitor of katanin was incorrect as this tail seemed to promote katanin severing during both preparations.

- The CTT β6, a construct with a large negative region and a bulky aromatic ring in the center, was predicted to be a good inhibitor of katanin. This construct presented another case of mixed results as it inhibited katanin well on 12-17-2015 but seemed to promote katanin severing on 3-24-2016. This tail needs to be retested.

- The CTT β1 has a large negative region along with a bulky aromatic group in the middle but contains a bulky, positively charged aromatic group at the end. Because of this bulky, positively charged aromatic group β1 was predicted to be a poor inhibitor of katanin. However, β1 was the best β-tail inhibitor of katanin severing.

- The E10 construct (a "tail" consisting of 10 glutamates) actually promoted katanin severing. Previous work on spastin, a member of the AAA+ severing enzyme family, has shown that polyglutamylation causes inhibition up to a certain point [23]. We find that the polyglutamylated construct actually causes activation of katanin severing resulting in a decrease in average severing time. Previous work with polyglutamylation was done using full length tubulin whereas we were working with a truncated tail version.

From our previous results, we expect that tubulin inhibits katanin through sequestration from the microtubule [3]. This means that CTT constructs that inhibit should result in a lower GFP-max along the microtubule and those that promote katanin severing should result in a higher GFP-max. What we find when looking at Figures 9 and 10 togetherr is that this is not necessarily the case:

- The CTT αδ2 was a very good inhibitor of katanin which means that it should have a lower GFP-max when compared to the control. However we see that the GFP-max is actually higher than the control for both preparations.

- This is also true for the CTT β A+Y.

- The CTT β2A is a good katanin inhibitor which should indicate a lower GFP-max, but this is only true for one of the preparations and not the other.

- The CTT β3, which showed promotion of katanin severing one day and inhibition on the other, is an interesting case. On 10-1-2015 β3 promoted katanin severing but had a GFP-max that was much lower than the control. The same tail on 11-24-2015 severely inhibited katanin severing but had a GFP-max that was higher than the control.

- The CTT β6 was the second tail that showed katanin severing promotion one day and katanin severing inhibition the next, but this tail had a lower GFP-max when compared to the control for both preparation days.

- The CTT β4B promoted katanin severing on both preparation days but had a GFP-max on both days that was slightly lower than the control.

- The CTT β1 inhibited katanin severing and behaved as predicted in regards to katanin binding to the microtubule, displaying reduced GFP-max compared to the control for both preparations.

- The E10 polypeptide promoted katanin severing on both days and had a resulting increase in GFP-max over the control, as expected.

CHAPTER 4

CONCLUSION

We have performed a preliminary quantitative investigation on the inhibitory effects of BSA-tubulin CTT constructs on katanin p60 severing and binding to microtubules. We have found that the chemical makeup of these tubulin CTT constructs affects the level of katanin severing and binding inhibition (Figures 9 and 10). Surprisingly, we found that free tubulin, which was previously shown in our lab to inhibit katanin severing and binding activity [3], appeared to result in an increased katanin activity in some of our assays (Figure 9). One possible explanation is that we used more katanin than in previous experiments, and an important factor is the katanin to inhibitor ratio. Future experiments will need to be performed to determine the relative concentration of katanin to CTT that will cause inhibition.

Another interesting result was that we found katanin appeared to be uninhibited by E10, a construct consisting of solely glutamates (Figure 9). This result was unexpected because polyglutamylation was previously shown to inhibit spastin, a different microtubule-severing enzyme [23]. This would be a second report displaying the functional differences between spastin and katanin with regard to the CTT sequences [2]. It implies that the recognition of tubulin is not the same between these two severing enzymes. They target and are inhibited by different tubulin sequences. This is important since they are expressed and active in different parts of cells and have different effects on the microtubule cytoskeleton, as shown time and

again [7, 19]. It is possible that removing the bulk of the tubulin protein affects how the CTT portion interacted with katanin, therefore altering the severing and binding inhibitory ability.

Understanding how cellular organization is controlled has far reaching implications for disease treatment and prevention. Katanin has been shown to act in a variety of cell types performing a number of important roles [19]. It could have a role in neuronal diseases, kidney disease, and cancer.

In terms of the research presented here, more tests of the CTTs should be conducted in order to get a better understanding of how they affect katanin severing and binding. The $\beta 3$ and $\beta 6$ tails, which had inconclusive results, need to be retested to get an idea of how they affect katanin. Further, all tail constructs should be tested during the same prep so that they can be compared to one another. This was just recently made possible by the finding that katanin could be stored at -20°C and -80°C in 50% for extended periods of time (1-2 weeks). This is long enough to be able to test all 8 tails using the same prep as well as any new constructs that we receive.

Figure 11:

Plots demonstrating data from experiments run on 11-24-2015. Four of the eight BSA-tubulin CTT constructs were tested and are listed along with the number of microtubules measured for each (N-Count) in the red box. All BSA tails tested were at 50nM concentration while katanin was present at 100nM. The zero control was a test performed to show that we were not photobleaching fluorophores during imaging. The left graph shows the differing rates of severing for each CTT tested by measuring average intensity along each individual microtubule as a function of time and combining all data for similar tests. The right graph shows binding profiles of katanin under different severing conditions by plotting average katanin intensity bound along the microtubule as a function of time. Light blue corresponds to the control of katanin alone, orange corresponds to the zero control photobleaching test, grey corresponds to the β2A CTT test, yellow corresponds to the αδ2 CTT test, purple corresponds to the β A+Y CTT test, and green corresponds to the β3 CTT test.

Figure 12:

Plots demonstrating data from experiments run on 12-17-2015. Four of the eight BSA-tubulin CTT constructs were tested and are listed along with the number of microtubules measured for each (N-Count) in the red box. All BSA tails tested were at 50nM concentration while katanin was present at 100nM. The zero control was a test performed to show that we were not photobleaching fluorophores during imaging. The left graph shows the differing rates of severing for each CTT tested by measuring average intensity along each individual microtubule as a function of time and combining all data for similar tests. The right graph shows binding profiles of katanin under different severing conditions by plotting average katanin intensity bound along the microtubule as a function of time. Orange corresponds to control katanin alone, light blue corresponds to the zero control photobleaching check, grey corresponds to the free tubulin test, yellow corresponds to the β4B CTT test, purple corresponds to the β6 CTT test, green corresponds to the β1 CTT test, and black corresponds to the E10 polyglutamate CTT test.
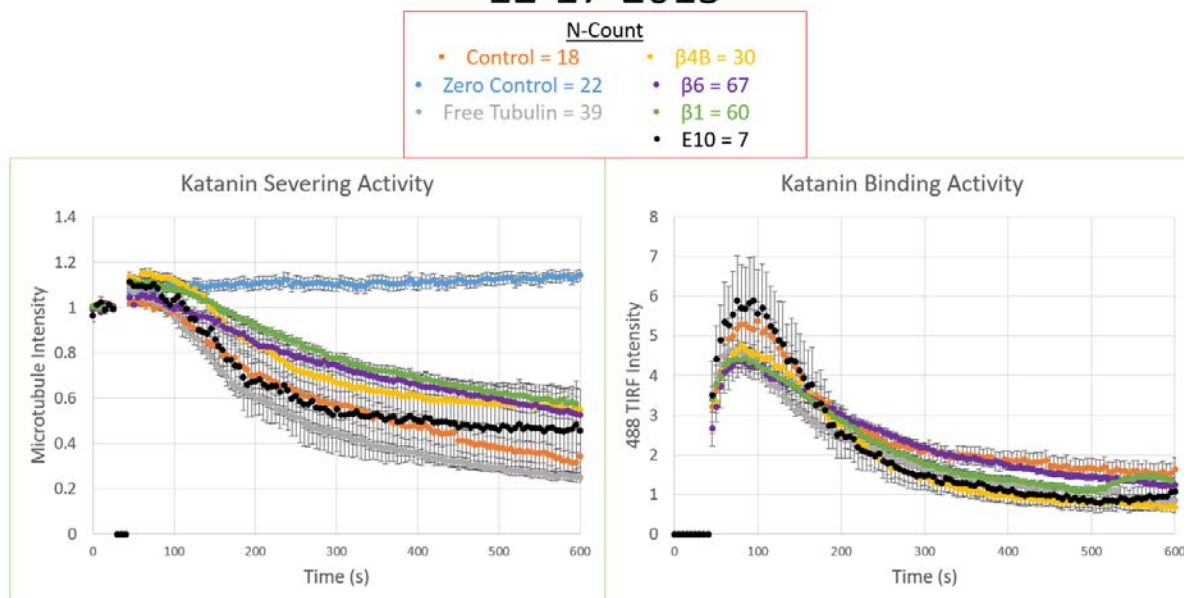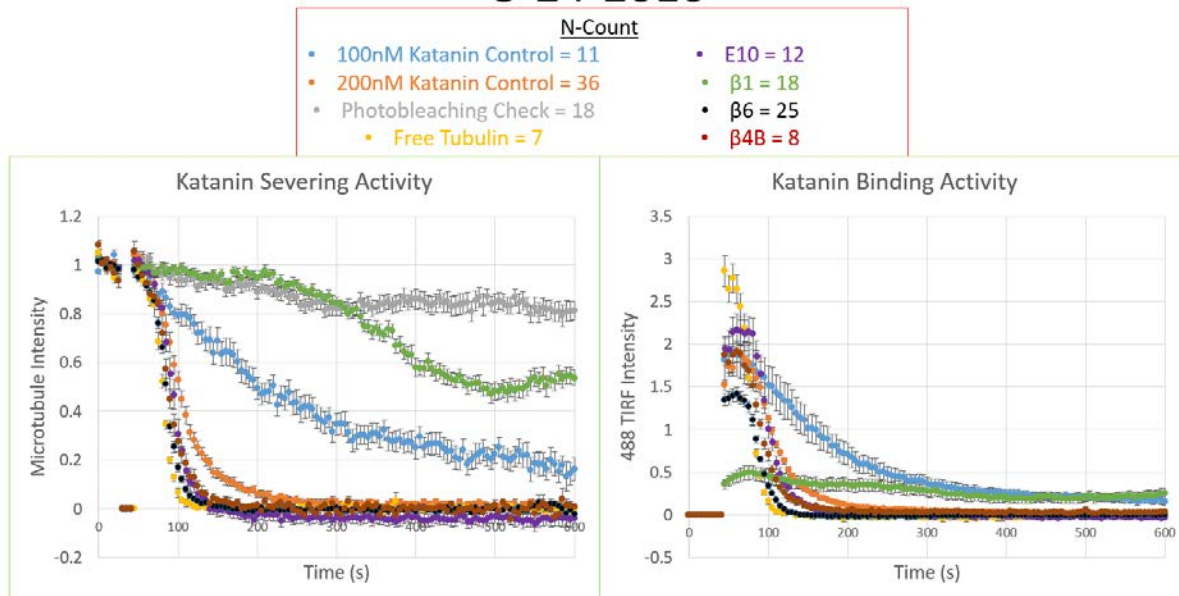
Figure 13:

Plots demonstrating data from experiments run on 3-24-2016. Four of the eight BSA-tubulin CTT constructs were tested and are listed along with the number of microtubules measured for each (N-Count) in the red box. All BSA tails tested were at 50nM concentration while katanin was present at 200nM during all inhibition tests. The zero control was a test performed to show that we were not photobleaching fluorophores during imaging. Two different concentrations of katanin are shown to display the difference in severing activity at different katanin concentrations. The left graph shows the differing rates of severing for each CTT tested by measuring average intensity along each individual microtubule as a function of time and combining all data for similar tests. The right graph shows binding profiles of katanin under different severing conditions by plotting average katanin intensity bound along the microtubule as a function of time. Light blue corresponds to the 100nM katanin control, orange corresponds to the 200nM katanin control, grey corresponds to the photobleaching check (zero control), yellow corresponds to the free tubulin test, purple corresponds to the E10 polyglutamate CTT test, green corresponds to the β1 CTT test, black corresponds to the β6 CTT test, and red corresponds to the β4B CTT test.

PROTOCOLS

B1: SDS-PAGE Protocol:

Gel Casting**:**

Resolving Gel (8%)	Stacking Gel (3.75%)
4.7 mL ddH_2O	3.1 mL ddH_2O
2.7 mL 30% acrylamide	625 μL 30% acrylamide
2.5 mL resolving buffer	1.25 mL stacking buffer
100 μL 10% SDS	50 μL 10% SDS
100 μL APS *	100 μL APS *
8 μL TEMED *	4 μL TEMED *

1. clean 2 sets of glass chambers for casting gel w/ 70% ETOH, dry completely

2. set up staging & test w/ ddH_2O for any leaks, fill completely (can leak from side tops), cleans inside from any leftover ETOH, dump in sink and dry as best as possible with filter paper

3. gather gel materials

   a. 30% acrylamide, 10% APS & TEMED in 4°

   b. resolving buffer, 10% SDS & isopropanol @ bench

4. mix ingredients for resolving gel in a 15 mL tube adding APS & TEMED last (they act as catalysts & cause the gel to solidify faster)

5. using Pasteur pipette put resolving gel into chambers up to bottom of staging, check if leaking (if it is, need to redo chamber)

6. top off chamber w/ isopropanol (levels out gel & removes bubbles)

7. let gel set for 30 – 45 minutes until completely solidified (check using leftovers in tube)

8. clean 2 combs w/ ETOH, dry completely

9. once resolving gel is solid, drain out isopropanol, rinse w/ ddH_2O & dry w/ filter paper

10. mix stacking gel in 15 mL tube, again adding APS & TEMED last

11. add stacking gel to chamber until it overflows slightly

12. insert combs, let solidify for 30 – 45 minutes until solid, check with leftovers

13. pull out chambers (glass plates), wrap each individually in a paper towel and place in a

    Tupperware container w/ an additional paper towel on top, soak completely in ddH_2O

    (this is only if storing overnight, if not, skip this step)

B2: Tubulin Purification from Pig Brains

<u>Stock Solutions:</u>

<u>PM Buffer (200mL)</u>   <u>PMG Buffer (200mL)</u>

200mM PIPES   100mL   76mL
200mM EGTA   2mL   2mL
100mM MgSO$_4$ 2mL   2mL
13.7M Glycerol   -------   116mL

<u>Super PMG (200mL)</u>

1M PIPES   16mL
1M MgSO$_4$ 2mL
200mM EGTA   2mL
13.7M Glycerol   175.2mL

1. Clean pig brains (3) and put in pre-tared 1L beaker

    Remove meniscus, etc. (use kimwipe to help clean)

2. Weigh cleaned brains: _____g

3. Put brains in blender

    Add 0.5mL PM buffer per 1g of brain. Volume of PM: _____mL

4. Pulse blender to homogenize brains (~5 seconds/pulse to prevent mixture from heating up)

5. Pour homogenized brains into ultra centrifuge tubes

6. Balance tubes

7. centrifuge at 100,000 xg for 45 minutes at 2°C with 50.2 Ti rotor

8. Pour supernatant into 500mL graduated cylinder (use pasteur pipette to get all sup)

    Volume of sup: _____mL

9. Add same volume of PMG to the sup (1:1 PMG:sup ratio)

*If sup volume is greater than 100mL, add ½ volume of sup as super PMG

10. Add GTP to final concentration of 1mM

_____mL of 100mM GTP stock

11. Cover graduated cylinder with parafilm and mix by inverting

12. Put sup into new ultra centrifuge tubes and balance

13. Polymerize MTs for 45 minutes at 37°C in water bath

14. Set ultra centrifuge to 37°C, place T865 rotor in 37°C incubator to warm up

15. Centrifuge at 100,000 xg in T865 rotor for 45 minutes at 37°C

These are the 1X Pellets (can drop freeze and store at -80°C or continue)

2X Pellets

1. Add PM to pellets using 1/5 volume of original homogenate (1X pellets, step 3)

Volume of PM Buffer added: _____mL

2. Using a thin, pointed spatula, scrape pellet off side of cfuge tube and into PM buffer

Lightly shake tube to make sure pellet is loose

Quickly dump PM buffer + pellet into 15mL dounce in ice slurry

Repeat for each pellet

3. Homogenize pellets in ice cold dounce until no large chunks seen (will be cloudy)

Homogenize on ice every 2-3 minutes, for a total of 30 minutes (avoid excessive

bubbling)

4. Put homogenized tubulin into ultra (T865) centrifuge tubes

5. Centrifuge 100,000 xg for 30 minutes at 2°C

6. Pour sup into graduated cylinder and approximate volume

   Volume of supernatant: _____mL

7. Add PMG buffer 1:1 with supernatant

   Add _____mL PMG

8. Add GTP to final concentration of 1mM

   Add _____ $\square$L 100mM GTP stock

9. Parafilm cylinder and mix by inverting

10. Put supernatant into new ultra T865 centrifuge tubes and incubate 45 minutes at 37°C in

    water bath

11. Centrifuge at 37°C for 45 minutes at 100,000 xg

12. Remove most of sup, leaving a small amount to cover pellets

13. Drop freeze pellets in liquid nitrogen and store at -80°C

High Salt Purification

1. Quickly thaw 2X pellets in 37°C water bath

2. Remove excess supernatant that froze with pellet

3. Take 2X pellets (2) and homogenize with dounce in 5mL PM buffer for 30 minutes on ice

   (Homogenize on ice every 2-3 minutes, for a total of 30 minutes, avoid excessive bubbling)

4. Spin at 100,000 xg at 4°C (T865 rotor) for 30 minutes

5. Save sup and add: 0.5 M PIPES
                       10% DMSO
                       1 mM GTP
                       2 mM EGTA
                       1 mM MgSO$_4$

6. Incubate at 37°C for 10 minutes

7. Spin 20 minutes at 20,000 xg at 37°C (T865 rotor)

8. Using dounce, homogenize pellet in 4mL PEM-100 on ice for 30 minutes

9. Spin 30 minutes at 100,000 xg at 4°C (T865 rotor)

10. Save supernatant as high salt purified tubulin

11. Bring tubulin to 5 mg/mL using PEM-100

12. Aliquot and drop freeze in liquid nitrogen, store in -80°C

B3: Severing Assay

* Chambers are assembled on glass slides that have been washed with 70% ethanol. Use doublestick tape to make a chamber with a silanized coverslip.

1. Flow in 2% anti-tubulin antibody (0.4 µL YL1/2 tubulin antibody + 9.6 µL PEM-100. Incubate 5 minutes.

2. Flow in 5% F-127. Incubate for 5 minutes.

3. Flow in 1:100 MTs. Incubate 5-7 minutes.

4. Flow in KAB-rxn #1 buffer.

5. Image 3 minutes.

6. Flow in Katanin in KAB-rxn buffer #2 (1:10 katanin:rxn buffer).

KAB-rxn Buffer 1:

2 µL	0.5% F-127
1 µL	DTT (1 M stock)
1 µL	BSA (100 mg/mL stock)
0.5 µL	Taxol (2 mM stock)
0.8 µL	ATP (50 mM stock)
1 µL	glucose (300 mg/mL stock)
1 µL	deoxy
12.7 µL	KAB
20 µL TOTAL	

KAB-rxn Buffer 2:

2 µL	0.5% F-127
1 µL	DTT (1 M stock)
1 µL	BSA (100 mg/mL stock)
0.5 µL	Taxol (2 mM stock)
0.8 µL	ATP (50 mM stock)
1 µL	glucose (300 mg/mL stock)
1 µL	deoxy
2 µL	Katanin (10x stock)
10.7 µL	KAB
20 µL TOTAL	

B4: Making Microtubules

1. Start centrifuge

    a. hit vacuum, make sure temp. set @ 4°C

2. Retrieve unlabeled and labeled tubulin from -80°C freezer, thaw aliquot in hands

    a. Cy5 tubulin doesn't need to be resuspended

    b. Rhodamine tubulin needs to be resuspended in 4μL of PEM100

3. Incubate aliquots on ice for 10min, while waiting:

4. Make desired concentration of unlabeled tubulin

    a. stock comes in aliquots of $9\frac{mg}{mL}$ but the desired concentration is $5\frac{mg}{mL}$

    b. $\left(9\frac{mg}{mL}\right)(10\mu L) = \left(5\frac{mg}{mL}\right)(10 + x) \rightarrow 90 = 50 + 5x \rightarrow 40 = 5x \rightarrow x = 8\mu L$

    c. 8μL is the amount of PEM100 to be added to the unlabeled tubulin stock to

    make the concentration $5\frac{mg}{mL}$

5. Retrieve 2 glass centrifuge tubes (in drawer left of Mike's desk)

6. Combine unlabeled and labeled tubulin in 1 glass centrifuge tube

    a. $(8\mu L\ PEM100 + 10\mu L\ unlabeled\ stock) + 10\mu L\ labeled\ stock =$

    $28\mu L\ total\ volume$

7. Fill second glass centrifuge tube with equal volume of ddH_2O, 28μL

8. Centrifuge tubes in the Sorvall Discovery M120 (near central desk where I sit) for 10 min

    @ 90,000 rpm to remove dead tubulin

    a. retrieve small rotor from 4°C fridge

    b. put centrifuge tubes in w/ labels facing out to help locate pellet when done

    c. settings: rotor #2, turn on vacuum (takes around 3 minutes to achieve full

       vacuum, 3 arrows)

9. Retrieve 10mM GTP from -20°C freezer (back left corner of room when walking in)

10. When centrifugation complete, remove the supernatant (careful to avoid the pellet) and

   relocate to 1.5mL Eppendorf tube.

    a. add 2.8µL of 10mM GTP to make a final concentration of 1mM GTP

11. Incubate Eppendorf tube in incubator (located near -20°C fridge in back left) for 20 min

   w/o shaking @ 37°C

12. Retrieve 2mM Taxol from -20°C fridge

13. Add 0.8µL of 2mM Taxol to tube so final concentration is 50µM of Taxol

    a. $(2000 \mu M \ stock \ taxol)(30.8 \mu L \ volume \ in \ Eppendorf \ tube) =$

      $(50 \mu M \ desired \ taxol \ concentration)(30.8 \mu L \ volume \ in \ Eppendorf \ tube +$

      $X \mu L \ volume \ of \ taxol \ to \ add) \rightarrow 61000 = 1540 + 50X \rightarrow 40 = 50X \rightarrow X =$

      0.8

14. Incubate another 20 min w/o shaking @ 37°C

15. Centrifuge Eppendorf tube using Eppendorf centrifuge (5415R on bench in lab) for 10

   min @ 25°C & 14,000 x gravity

16. Remove & discard supernatant, resuspend pellet in a solution of 50µM taxol and

   PEM100 so that the final volume is 28µL

    a. $(2000 \mu M \ [taxol] original)(X \mu L \ taxol \ added) =$

      $(50 \mu M \ [taxol] desired)(28 \mu L \ volume \ desired) \rightarrow 2000X = 1400 \rightarrow X = 0.7$

    b. 0.7µL of taxol & 27.3µL of PEM100 added

17. Incubate @ 37°C w/o shaking for full day

B5: Silanization of Coverslips:

*It is important to clean the racks and glass containers thoroughly before silanization.

*Do not let anything that is not dry come in contact with the silane.

*Rinse container 3X with water then 3X with ddH$_2$O for each step.

Clean Coverslips:

1. Immerse the coverslips in 100% acetone for 1 hour.

2. Immerse the coverslips in 100% ethanol for 10 minutes.

3. Rinse 3X in ddH$_2$O for 5 minutes each.

4. Immerse the coverslips in 0.1M KOH for 15 minutes (prepare just before use).

5. Rinse 3X in ddH$_2$O for 5 minutes each.

6. Air Dry Coverslips.

Silanization of Coverslips:

1. Once cleaned coverslips have dried completely, immerse in 2% DDS (dimethyldichlorosilane)

   for 5 minutes.

2. Use a funnel to pour the silane solution back into the bottle to reuse.

3. Immerse the coverslips in 100% ethanol for 5 minutes.

4. Immerse the coverslips in another 100% ethanol for 5 minutes.

5. Rinse 3X in ddH$_2$O for 5 minutes each.

Air Dry.

B6: Bacterial Katanin Purification

Resuspension Buffer:
20mM Hepes pH 7.7
250mM NaCl
10% Glycerol
0.5 mM MgATP pH 7
1mM PMSF
Protease Inhibitors:
      2 mg/mL Aprotinin
      2 mg/mL Pepstatin
      2 mg/mL Leupeptin

Katanin Activity Buffer:
20 mM Hepes pH 7.7
2 mM $MgCl_2$
10% Glycerol

Day 1:

Transform p60 into BL21 cells. Plate on Amp plates.

Day 2:

Pick 3 colonies and start 3 overnight start cultures with Ampicillin and   Chloramphenicol. Make

up 3x 500 mL of LB. 1 L LB: 10 g NaCl   10 g tryptone   5 g yeast extract

Day 3:

(A) Add Ampicillin and Chloramphenicol to flasks of LB. Antibiotics are made up for a 1:1000

dilution into cultures. (B) Add starter cultures to flasks of LB. Should be 1:100 dilution so for 1 L

add 10 mL of starter culture. (C) Grow cultures in shaking incubator at 37 C until it reaches an

O.D. of 0.8. This usually   takes about 6 hours. (D) Add 1 mM IPTG (1 M stock) to the culture.

Bring the culture to Tom Maresca's Lab and grow in the shaker at 16 C for 15-18 hours. Lab

code: 7995

Day 4:

Pellet bacteria at 5,000 rpm for 15 min. DO NOT FREEZE. 2. Make up 50ml of resuspension buffer.   *Remember to add Protease inhibitors as well. 1. Resuspend pellets in 15 ml of Resuspension Buffer. 2. Lyse cells using the sonicator every 20 seconds for 20 seconds for a total of 3 minutes. 3. Transfer sonicated lysate to red capped centrifuge tube. 4. Centrifuge in T865 at 13,000 rpm for 30 minutes. 5. Incubate lysate with ~1 ml bed volume of amylose resin for ~1.5-2 hours at 4C.

 *Wash resin before in column/resuspension buffer 3x. 2x with water, 1x   with resuspension buffer at 3,000 RPM for 5 minutes each. 1. Pour lysate into column and wash with ~20 mL of resuspension buffer. 2. Elute with 10 mM Maltose in resuspension buffer (50 µL of 1 M maltose to 5mL of completed resuspension buffer). Perform bradford to get concentration.

BIBLIOGRAPHY

(1) "About Tubulin." *Cytoskeleton*, 2015, www.cytoskeleton.com/about/tubulin. Accessed 11
Aug. 2016.

(2) Bailey, Megan E. *Biophysical Characterization of Katanin's Regulation of Microtubules*. 2015.
U of Massachusetts Amherst, PhD dissertation.

(3) Bailey, Megan E., Dan L. Sackett, and Jennifer L. Ross. "Katanin Severing and Binding
Microtubules Are Inhibited by Tubulin Carboxy Tails." *Biophysical Journal* 109 (2015):
2546-61. Print.

(4) Bailey, Megan E., et al. "Microtubule Severing Enzymes Couple ATPase Activity with Tubulin
GTPase Spring Loading." *Biopolymers* (2016): n. pag. Print.

(5) Connell, James W., Rachel Allison, and Evan Reid. "Quantitative Gait Analysis Using a
Motorized Treadmill System Sensitively Detects Motor Abnormalities in Mice
Expressing ATPase Defective Spastin." *PLOS ONE* (2016): 1-16. Print.

(6) Davis, Liza J., et al. "The Importance of Lattice Defects in Katanin-Mediated Microtubule
Severing in Vitro." *Biophysical Journal* 82 (2002): 2916-27. Print.

(7) Eckert, Thomas, et al. "Spastin's Microtubule-Binding Properties and Comparison to
Katanin." *PLOS ONE* 7.12 (2012): 1-16. Print.

(8) Eckert, Thomas, et al. "Subunit Interactions and Cooperativity in the Microtubule-severing
AAA ATPase Spastin." *The Journal of Biological Chemistry* 287.31 (2012): 26278-90.
Print.

(9) Fojo, Tito, and Beverly A. Teicher, editors. *The Role of Microtubules in Cell Biology,
Neurobiology, and Oncology*. Totowa, Humana Press, 2008. Cancer Drug Discovery
and Development.

(10) Hartman, James J., et al. "Katanin, a Microtubule-Severing Protein, Is a Novel AAA ATPase
that Targets to the Centrosome Using a WD40-Containing Subunit." *Cell* 93 (1998):
277-87. Print.

(11) Hartman, James J., and Ronald D. Vale. "Microtubule Disassembly by ATP-Dependent Oligomerization of the AAA Enzyme Katanin." *Science* 286 (1999): 782-85. Print.

(12) Mace, Alex, and Wenjia Wang. "Modelling the role of catastrophe, crossover and katanin-mediated severing in the self-organisation of plant cortical microtubules." *The Institution of Engineering and Technology* 9.6 (2015): 277-84. Print.

(13) McNally, Francis J., and Ronald D. Vale. "Identification of Katanin, an ATPase That Severs and Disassembles Stable Microtubules." *Cell*, vol. 75, 5 Nov. 1993, pp. 419-29.

(14) Peng, Wentao, et al. "Structural Insights into the Unusually Strong ATPase Activity of the AAA Domain of the Caenorhabditis elegans Fidgetin-like 1 (FIGL-1) Protein." *The Journal of Biological Chemistry* 288.41 (2013): 29305-12. Print.

(15) Roll-Mecak, Antonina, and Ronald D. Vale. "Structural basis of microtubule severing by the hereditary spastic paraplegia protein spastin." *Nature*, 17 Jan. 2008, pp. 363-67.

(16) Ross, Jennifer L., and Ram Dixit. "Multiple Color Single Molecule TIRF Imaging and Tracking of MAPs and Motors." *Methods In Cell Biology*, vol. 95, 2010, pp. 521-54.

(17) Ross, Jennifer L. "Research." *Ross Lab, Department of Physics, University of Massachusetts Amherst*, edited by Jennifer L. Ross, Jennifer L. Ross, www.rosslabbiophysics.com/#!research/cswb. Accessed 11 Aug. 2016.q

(18) Selcuk, Ece, et al. "Katanin-p80 Gene Promoter Characterization and Regulation via Elk1." *PLOS ONE* 8.7 (2013): 1-13. Print.

(19) Sharp, David J., and Jennifer L. Ross. "Microtubule-severing enzymes at the cutting edge." *Journal of Cell Science* 125 (2012): 2561-69. Print.

(20) Sudo, Haruka, and Peter W. Baas. "Strategies for diminishing katanin-based loss of microtubules in tauopathic neurodegenerative diseases." *Oxford Journals*, vol. 20, no. 4, 30 Nov. 2010, pp. 763-78.

(21) Taylor, Jennifer L., et al. "Crystal structure of the human spastin AAA domain." *Journal of Structural Biology* 179 (2012): 133-37. Print.

(22) Vale, Ronald D. "Severing of Stable Microtubules by a Mitotically Activated Protein in Xenopus Egg Extracts." *Cell*, vol. 64, 22 Feb. 1991, pp. 827-39.

(23) Valenstein, Max L., and Antonina Roll-Mecak. "Graded Control of Microtubule Severing by Tubulin Glutamylation." *Cell* 164 (2016): 911-21. Print.

(24) White, Susan Roehl, et al. "Recognition of C-terminal amino acids in tubulin by pore loops in Spastin is important for microtubule severing." *The Journal of Cell Biology* 176.7 (2007): 995-1005. Print.